

Unfolding AlphaFold’s Bayesian Roots in Probability Kinematics

Thomas Hamelryck
University of Copenhagen, Denmark
thamelry@bio.ku.dk

Kanti V. Mardia
University of Leeds, UK
K.V.Mardia@leeds.ac.uk

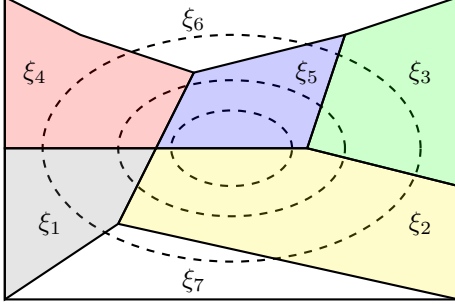
Abstract

We present a novel theoretical interpretation of AlphaFold1 that reveals the potential of generalized Bayesian updating for probabilistic deep learning. The seminal breakthrough of AlphaFold1 in protein structure prediction by deep learning relied on a learned potential energy function, in contrast to the later end-to-end architectures of AlphaFold2 and AlphaFold3. While this potential was originally justified by referring to physical potentials of mean force (PMFs), we reinterpret AlphaFold1’s potential as an instance of *probability kinematics* — also known as *Jeffrey conditioning* — a principled but under-recognised generalization of conventional Bayesian updating. Probability kinematics accommodates uncertain or *soft* evidence in the form of updated probabilities over a partition. This perspective reveals AlphaFold1’s potential as a form of generalized Bayesian updating, rather than a thermodynamic potential. To confirm our probabilistic framework’s scope and precision, we analyze a synthetic 2D model in which an angular random walk prior is updated with evidence on distances via probability kinematics, mirroring AlphaFold1’s approach. This theoretical contribution connects AlphaFold1 to a broader class of well-justified Bayesian methods, allowing precise quantification, surpassing merely qualitative heuristics based on PMFs. Our contribution is theoretical: we replace AlphaFold1’s heuristic analogy with a principled probabilistic framework, tested in a controlled synthetic setting where correctness can be assessed. More broadly, our results point to the considerable promise of probability kinematics for probabilistic deep learning, by allowing the formulation of complex models from a few simpler components.

1 Introduction

The protein structure prediction problem – predicting the three-dimensional (3D) structure of a protein from its amino acid sequence – has been a central unsolved challenge in molecular biology for more than 50 years [17]. In 2024, the shared Nobel Prize in Chemistry was awarded to John Jumper and Demis Hassabis for AlphaFold’s solution of this problem [10]. Here, we focus on the initial formulation of AlphaFold, which we will refer to as AlphaFold1 (AF1) [55, 56]. AF1 differs considerably from the end-to-end prediction approach of its two successors [34, 1] in that it makes use of a potential function parameterized by deep learning. Predictions by AF1 are obtained from minimizing this potential energy function. We propose here that AF1’s general approach is well worth reconsidering as a basis for further development, as we discuss below.

AF1’s potential function was justified by qualitative analogy to physical *potentials of mean force* (PMFs) [55, 56] as used in the physics of liquids, first formulated by Kirkwood in 1935 [37]. Here, we show instead that AF1 is an instance of an under-recognized generalization of Bayesian updating called *Jeffrey conditioning* or *probability kinematics* (PK). PK was introduced by the philosopher of logic and probability Richard C. Jeffrey in 1957 [31, 32, 33], and specifies how to incorporate *soft*



$$\begin{aligned}
 (A) \quad & \pi(\omega) = \sum_i \pi(\omega \mid \xi_i) \pi(\xi_i), \\
 (B) \quad & p(\omega \mid \xi_i) = \pi(\omega \mid \xi_i) \\
 (C) \quad & \Rightarrow p(\omega) = \sum_i \pi(\omega \mid \xi_i) p(\xi_i) \\
 (D) \quad & \Rightarrow p(\omega) = \frac{p(\xi(\omega))}{\pi(\xi(\omega))} \pi(\omega)
 \end{aligned}$$

Figure 1: **Schematic example of PK for the case of a finite partition.** The dotted lines denote the equiprobability contours of the probability density function (PDF) of a prior distribution, $\pi(\omega)$, defined on a rectangle. The solid lines represent a finite partition $\{\xi_i\}$ of the support of $\pi(\omega)$, with probabilities $\{\pi(\xi_i)\}$. $\pi(\omega)$ can thus be written as in (A). New evidence is then obtained in the form of updated probabilities for the partition, $\{p(\xi_i)\}$. PK updates the prior $\pi(\omega)$ to the posterior $p(\omega)$ by keeping the conditional following (B), which is called the *Jeffrey-condition* or *J-condition*, and replacing the marginal as in (C). The equivalent expression (D), where $\xi(\omega)$ is the partition element that contains ω , is obtained by applying Bayes’ formula. The latter form, called the *Reference Ratio* (RR) update, is of interest when the conditional in (C) is not readily available or tractable, as is the case for AF1. PK readily generalizes to infinite partitions (see Section 3).

evidence in the form of updated probabilities on a partition of a random variable (see Figure 1), rather than a concrete event. AF1 updates an empirical Bayes prior over protein dihedral angles with soft evidence on pairwise distances between amino acids, both obtained from deep models.

This theoretical paper offers the following contributions:

- Building on a definition of PK for PDFs and infinite partitions tailored to the case of AF1, we propose a generalized Bayesian reinterpretation of AF1’s potential function.
- We contrast our framework with AF1’s heuristic explanation based on PMFs and link its deep model to statistical models of protein structure. This bridge is timely, as there is a growing need for modelling epistemic and aleatoric uncertainty [9, 53, 11, 2, 21, 12, 42].
- We introduce a tractable two-dimensional synthetic model that is analogous to AF1’s potential. The model updates an angular prior with evidence in the form of a PDF over a distance. This setup mirrors the probabilistic framework behind AF1’s potential and allows us to demonstrate the update’s precision via hypothesis testing.
- We reveal PK as a previously unrecognised foundation for formulating deep generative models of biomolecular structure.
- Our results show PK’s relevance and potential in formulating *compositional* deep generative models, ie. models constructed by combining simpler probabilistic components into a coherent whole [22, 69, 6].

Our aim is not to improve or assess empirical accuracy, as AF1’s historical success is well established [55, 56], but to clarify its previously unrecognized statistical foundation. To do this, we replace AF1’s heuristic analogy with a principled probabilistic framework, tested in a controlled synthetic setting where correctness can be assessed.

2 Background

2.1 Preliminaries

Notation and assumptions We will use the following generic notation to emphasize features common to PK and PMFs. Let ω be a random variable, and let ξ be a random variable obtained via a many-to-one mapping, $\xi(\omega)$. Thus, ξ is a random variable and $\xi(\omega)$ is the specific *realization* of ξ for a given value of ω . We will call ω a *fine-grained* random variable, and ξ a corresponding *coarse-grained* or *collective* random variable. Depending on the context, ω and ξ may be vector-valued,

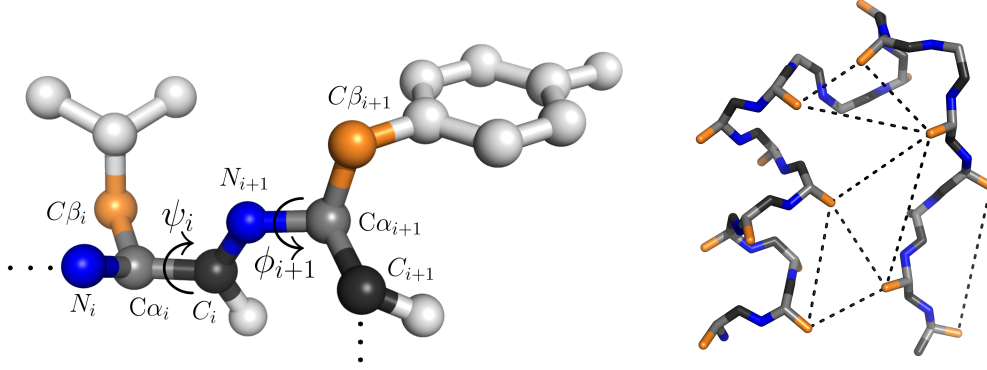


Figure 2: **(left)** Two amino acids in a protein, with relevant atoms and dihedral angles labeled. Atoms that do not play a role in the AF1 potential, including side chain and backbone oxygen atoms, are shown in white. The continuation of the protein backbone is indicated with dots. **(right)** A protein (Protein Data Bank identifier 1L2Y) with a subset of all the $C\beta - C\beta$ distances shown in black dotted lines. Only the atoms relevant to the AF1 potential are shown. Figures made with PyMol [54].

scalar or discrete; in the latter two cases we omit the boldface for clarity. These symbols are reused and explained in their context as needed.

The protein amino acid sequence, s , of length L , is represented by a $20L$ vector of concatenated 20-dimensional one hot encodings of the 20 amino acid symbols. M is an $M \times 20L$ matrix that contains the multiple sequence alignment of M protein sequences related to s . A protein structure will be represented by its backbone atoms only, including $N, C\alpha, C, C\beta$ atoms (see Figure 2). The 3D coordinates of these four atoms for each amino acid are contained in the tensor, \mathbf{X} , which is $L \times 4 \times 3$.

Protein structure is often parameterized using dihedral angles,¹ which has the advantage of invariance to rotation and translation and statistical simplicity [26]. Let ϕ and ψ be vectors of L dihedral angles in $[-\pi, \pi]$. These vectors establish a rotation-invariant representation of the coordinates – we will write $\mathbf{X}(\phi, \psi)$, where \mathbf{X} is determined by the angles up to an arbitrary rotation and translation. Following AF1 [55, 56], we will assume ideal bond angles, ideal bond lengths, the third backbone dihedral angle $\omega = \pi$ for all amino acids, and ignore amino acid side chains and the backbone oxygen atom, without any loss of generality (see Figure 2).

Let the random variable D represent the $L \times L$ distance matrix of distances between L $C\beta$ atoms, with $L(L-1)/2$ unique values. Note that although these pairwise distances only involve the $C\beta$ atoms, they are taken as representative distances between amino acids. A given set of atomic coordinates, \mathbf{X} , or dihedral angles, (ϕ, ψ) , determines D fully – we will write $D(\mathbf{X})$ and $D(\phi, \psi)$ for the concrete realization of D for given coordinates or dihedral angles. NN will denote a neural network.

2.2 AF1’s potential

AF1’s potential contains four terms, three of which are parameterized by deep models. A fourth, repulsive potential is derived from physical considerations and merely serves to prevent atoms from overlapping. The first three potentials are central to this article. The exact form of the PDFs mentioned below will be detailed in Section 4.

The first potential concerns the dihedral angles and is given by

$$V_{\text{Dihedral}}(\phi, \psi) = - \sum_i \log p(\phi_i, \psi_i \mid s, M). \quad (1)$$

¹A *dihedral angle* or *torsion angle*, defined by four consecutively bonded atoms, is the angle between the planes formed by the first three atoms and the last three. Under the common assumption that bond lengths and bond angles take fixed, ideal values, a protein’s 3D structure can be fully parameterized by its set of backbone and side-chain dihedral angles.

where the sum runs over all amino acids. The second energy terms contains the pairwise distances between the $C\beta$ atoms, which serve as representative distances between amino acids i and j ,

$$V_{\text{Distance}}(\mathbf{D}) = - \sum_{i,j,i \neq j} \log p(D_{i,j} | \mathbf{s}, \mathbf{M}). \quad (2)$$

As we will show in Section 4, the formulation of a consistent joint probability distribution over angles and distances requires a third term – a so-called *reference potential*, which also concerns pairwise distances. This potential depends only on the length of the sequence, $L(\mathbf{s})$, and a one-hot vector that specifies the positions of Glycine residues, $\mathbb{I}_{\text{Glycine}}(\mathbf{s})$. Glycine is a small amino acid that allows exceptional conformational freedom to the protein chain. The reference potential is

$$V_{\text{Reference}}(\mathbf{D}) = - \sum_{i,j,i \neq j} \log p(D_{i,j} | L(\mathbf{s}), \mathbb{I}_{\text{Glycine}}(\mathbf{s})). \quad (3)$$

What AF1 refers to as a PMF is then obtained from their difference,

$$V_{\text{PMF}}(\mathbf{D}) = V_{\text{Distance}}(\mathbf{D}) - V_{\text{Reference}}(\mathbf{D}). \quad (4)$$

The final potential brings the three potential above together, and combines it with the predefined repulsive potential,

$$V_{\text{AF1}}(\phi, \psi) = V_{\text{PMF}}(\mathbf{D}(\phi, \psi)) + V_{\text{Dihedral}}(\phi, \psi) + V_{\text{Repulsive}}(\mathbf{X}(\phi, \psi)). \quad (5)$$

Note that \mathbf{D} and \mathbf{X} (up to an arbitrary rotation) in the above expression are fully determined by the dihedral angles, ϕ and ψ (see Figure 2). Prediction by AF1 amounts to minimizing the potential as a function of the dihedral angles using gradient descent. In the next section, we explain how AF1 justifies this potential by heuristic analogy with PMFs for liquid systems.

2.3 AF1’s potential justified as a PMF

Physical potentials of mean force A PMF can be understood as an "averaged", "mean" or "effective" potential regarding some coordinates (typically called the *collective or coarse-grained variables*) of a physical system, while averaging over the remaining degrees of freedom [14, 72, 28]. A PMF is defined as

$$p(\xi) \propto \exp(-\text{PMF}(\xi)/kT) = \int \delta(\xi - \xi(\mathbf{X})) \exp(-U(\mathbf{X})/kT) d\mathbf{X}, \quad (6)$$

where k is Boltzmann’s constant, T is the temperature, \mathbf{X} are the atomic coordinates of the system, ξ is the collective random variable, $\xi(\mathbf{X})$ is the realization of ξ at \mathbf{X} , $\delta(\cdot)$ is the Dirac delta function, and the exponential factor is the Boltzmann distribution associated with internal energy U .

PMFs were introduced by Kirkwood in his seminal paper from 1935 [37], applied to mixtures of liquids. What is relevant here is that Kirkwood potentials give rise to expressions of the form,

$$\text{PMF}_K(r) = -kT \log \left(\frac{p(r)}{p_R(r)} \right), \quad (7)$$

where r is the distance between two liquid particles. The numerator in the log is the probability density observed in a liquid, while the denominator refers to a so-called *reference distribution*. In the case of Kirkwood PMFs, the reference distribution is well-defined, corresponding to an ideal state of non-interacting particles [37]. We now turn to the heuristic adoption of formulas similar to Kirkwood PMFs, as done by AF1, for biomolecular prediction and simulation.

Knowledge based potentials Knowledge based potentials (KBPs) attempt to formulate empirical energy functions based on statistics derived from the database of known structures [52, 64, 49, 58]. KBPs based on the pairwise distances between $C\beta$ atoms were introduced in Sippl (1990) [58] and widely adopted [61, 59, 62]. The energy of a protein structure following such a KBP is given by

$$\Delta e_s(\mathbf{X}) = \sum_{i < j} -\log \left(\frac{p(D_{i,j}(\mathbf{X}) | s_i, s_j)}{p_R(D_{i,j}(\mathbf{X}) | s_i, s_j)} \right), \quad (8)$$

These potentials were formulated by qualitative analogy with the Kirkwood PMFs discussed in the previous section. Despite undisputed success, their theoretical justification as PMFs was widely

contested [65, 5, 38]. Notably, unlike physical PMFs, KBPs are not derived from a Boltzmann distribution of a single system, but from a heterogeneous data set of different protein structures, and the reference distribution is undefined [5, 38]. Attempts at qualitative justification invoked properties of random polymers [20] and probabilistic reasoning [57]. Subsequently, pairwise KBPs were quantitatively explained [25, 67], and eventually recognised as an instance of PK [27], to which we turn next.

2.4 Probability kinematics

As in the classic example of *Whitworth's horses* [16] (see Appendix 9), new information often does not arrive in the form of a deterministic event, but rather as a revision in the probability of various hypotheses. PK provides a framework for updating beliefs under such uncertain evidence. Unlike classical Bayesian conditioning, which updates a prior $\pi(\omega)$ to a posterior $p(\omega) \propto p(\mathbf{y} | \omega)\pi(\omega)$ where \mathbf{y} is observed data, PK updating uses revised probabilities on a partition of ω (Figure 1).

Given a prior distribution $\pi(\omega)$ over a sample space Ω , and a finite partition $\{\xi_i\}$ of Ω along with new marginal probabilities $p(\xi_i)$ that differ from the prior probabilities $\pi(\xi_i)$, the PK update prescribes the posterior as

$$p(\omega) = \sum_i \pi(\omega | \xi_i) p(\xi_i), \quad (9)$$

when the conditional probabilities remain unchanged, i.e., $p(\omega | \xi_i) = \pi(\omega | \xi_i)$. This condition is referred to as the *Jeffrey condition* or *J-condition*.

Unlike conventional Bayesian inference, PK does not rely on an explicit likelihood function, and its evidence is not a concrete event. Nonetheless, PK preserves essential features of Bayesian updating. First, PK satisfies the Dutch book argument [3]. Second, PK reduces to conventional Bayesian updating when for one of the partition elements, $p(\xi_i) = 1$. Third, among all distributions that match the updated marginals $\{p(\xi_i)\}$, the PK update minimizes the Kullback-Leibler divergence to the prior π [16]. This links the method to a variational principle [7, 36] that fits the Bayesian interpretation of probability [16]. PK is usually formulated in terms of probabilities and finite partitions [48]. In the next section, we outline the more general probabilistic framework needed to address the AF1 case.

3 Probabilistic framework

In this section, we first formulate a definition of PK that is suitable for our purposes (i.e., concerning PDFs and infinite partitions), and review some of PK's properties. As a preliminary to its application in the case of AF1, we consider the case of pairwise distance KBPs and contrast PK with physical PMFs.

3.1 PK for the case of PDFs and infinite partitions

We provide a simplified definition tailored to the present case based on [16] and [48], while avoiding the formalism of measure theory and irrelevant boundary cases.

Definition 1 (Probability Kinematics for Infinite Partitions and PDFs). *Given:*

- A random variable $\omega \in \Omega$, where Ω is a smooth manifold (e.g., the m -torus \mathbb{T}^m), equipped with a prior density $\pi(\omega)$.
- A random variable ξ , where ξ can be written as a many-to-one function $\xi(\omega)$ of ω , taking values in a smooth manifold Ξ (e.g., the space of valid pairwise distances between n points in \mathbb{R}^k), forming an **infinite partition** of Ω . Its prior density $\pi(\xi)$ is induced by $\pi(\omega)$ via

$$\pi(\xi) = \int \delta(\xi(\omega) - \xi) \pi(\omega) d\omega. \quad (10)$$

Each value $\xi \in \Xi$ defines a partition element: the set $\{\omega \in \Omega : \xi(\omega) = \xi\}$.

- **Evidence** as a new density $p(\xi)$ (e.g., regarding pairwise distances between amino acids).
- Densities $\pi(\xi)$ and $p(\xi)$ are positive on a common support and normalized. We will call ω and ξ the **fine-grained** and the **coarse-grained or collective** random variables, respectively.

- We assume all functions and densities are sufficiently well-behaved to ensure the existence and measurability of the integrals and conditional densities involved.

A **probability kinematics** update defines a posterior density $p(\omega)$ by satisfying the following conditions, which together ensure the evidence is incorporated while preserving conditional distributions:

1. **Faithfulness:** The marginal density of ξ matches the evidence,

$$p(\xi) = \int p(\omega) \delta(\xi(\omega) - \xi) d\omega. \quad (11)$$

2. **J-Condition:** The conditional density of ω given ξ is preserved,

$$p(\omega | \xi) = \pi(\omega | \xi). \quad (12)$$

3. **Update Rule:** The posterior $p(\omega)$ is obtained as,

$$p(\omega) = \int \pi(\omega | \xi) p(\xi) d\xi = \pi(\omega | \xi(\omega)) p(\xi(\omega)), \quad (13)$$

4. **Reference Ratio (RR) Update Rule:** Equivalently, after applying Bayes' formula to (13),

$$p(\omega) = \int \frac{\delta(\xi - \xi(\omega)) \pi(\omega)}{\pi(\xi)} p(\xi) d\xi = \frac{p(\xi(\omega))}{\pi(\xi(\omega))} \pi(\omega). \quad (14)$$

The Dirac delta function arises from the fact that $p(\xi | \omega) = \delta(\xi - \xi(\omega))$. Note that (14) follows directly from the J-condition given by (12).

Consequence: The posterior $p(\omega)$ has marginal $p(\xi)$ and preserves the conditional $\pi(\omega | \xi)$.

3.2 KBPs versus PMFs

KBPs can be understood as an application of PK [25, 47, 67, 27]. Consider a prior distribution over protein structure, $\pi(\mathbf{X})$. Without any loss of generality, we leave out the conditioning on sequence. We are now given soft evidence about pairwise distances between amino acids, $p(\mathbf{D})$, say, only involving $C\beta$ atoms. Thus, the collective random variable \mathbf{D} pertains to a subset of atoms, induces a partition on the space of \mathbf{X} , and corresponds to ξ in Definition 1. By construction, the J-condition holds, that is, $p(\mathbf{X} | \mathbf{D}) = \pi(\mathbf{X} | \mathbf{D})$. In other words, if we sample an infinite number of structures from the prior and retain those with a specified \mathbf{D} , we would get samples from the desired distribution $p(\mathbf{X} | \mathbf{D})$. The PK update following (14) is then given by

$$p(\mathbf{X}) = \int \frac{\delta(\mathbf{D}(\mathbf{X}) - \mathbf{D}) \pi(\mathbf{X})}{\pi(\mathbf{D})} p(\mathbf{D}) d\mathbf{D} = \frac{p(\mathbf{D}(\mathbf{X}))}{\pi(\mathbf{D}(\mathbf{X}))} \pi(\mathbf{X}). \quad (15)$$

Note that \mathbf{D} is a random variable, while $\mathbf{D}(\mathbf{X})$ is its realisation at \mathbf{X} . A minus-log transform recovers the KBP given by (8),

$$\Delta e(\mathbf{X}) = -\log \left(\frac{p(\mathbf{D}(\mathbf{X}))}{\pi(\mathbf{D}(\mathbf{X}))} \right) - \log(\pi(\mathbf{X})), \quad (16)$$

if we assume conditional independence of pairwise distances (see also Appendix 11). The additional second term does not appear in standard KBP expressions, as it is typically implicitly accounted for by Monte Carlo sampling [57] or scoring of existing structures [60].

The contrast of KBPs with PMFs is now obvious: while PMFs amount to a projection and marginalization of a well-defined Boltzmann distribution for a single physical system as in (6), KBPs as in (16) correspond to a generalized Bayesian update of an (empirical) prior by means of PK. PK and PMFs produce distributions over fine- and coarse-grained variables, respectively. What they *do* have in common is a Dirac delta function that projects a fine-grained variable onto a coarse-grained observable. We now show that AF1 can be understood from the perspective of PK.

4 AF1’s potential re-evaluated

4.1 AF1’s potential as an instance of PK

In this section, we present a reformulation of the AF1 potential in probabilistic terms. First, we reinterpret the potential over the dihedral angles as an empirical prior that is updated with soft evidence on pairwise distances. Building on previous work concerning probabilistic models over dihedral angles [19, 24, 8, 39, 71, 40] based on directional statistics [46, 41, 51, 43, 44], this prior is formulated as

$$\pi(\phi, \psi; \Theta) = \prod_i \text{vonMises}(\phi_i; \Theta_i) \text{vonMises}(\psi_i; \Theta_i), \quad (17)$$

where the parameters are obtained from a deep model, $\Theta = \text{NN}_{\text{Dihedral}}(s, M)$, and vonMises is the von Mises distribution. This circular distribution is analogous to a Gaussian distribution and suitable for modeling dihedral angles in $[-\pi, \pi]$ [46]. The prior over dihedral angles implies a matching prior over distances,

$$\pi(D; \Gamma) \propto \prod_{i,j,i \neq j} p(D_{i,j}; \Gamma_{i,j}), \quad (18)$$

where $\Gamma = \text{NN}_{\text{Reference}}(L(s), \mathbb{I}_{\text{Glycine}}(s))$.

The local prior will be updated with soft evidence on distances following the generalized Bayesian approach of PK. The updated probability distribution over the distances is,

$$p(D; \Omega) \propto \prod_{i,j,i \neq j} p(D_{i,j}; \Omega_{i,j}), \quad (19)$$

where $\Omega = \text{NN}_{\text{Distance}}(s, M)$. We now have all the elements in place to invoke the machinery of probability kinematics. Following PK’s RR update given by (14), the posterior is obtained as

$$p(\phi, \psi; \Theta, \Gamma, \Omega) \propto \frac{p(D(\phi, \psi); \Omega)}{\pi(D(\phi, \psi); \Gamma)} \pi(\phi, \psi; \Theta). \quad (20)$$

By construction and following [8, 67], AF1 adopts the J-condition induced by a prior over dihedral angles. Why is the PK update needed, if dihedrals angles are in principle sufficient to determine the structure? The answer is well known: due to an elbow effect, the dihedral prior is accurate for residues that are close in sequence position, but becomes increasingly unreliable for residues that are distant [30, 23]. This *locality* is a well-known limitation of probabilistic models based on dihedral angles, and is due to the accumulation of small errors [4]. In AF1, PK provides a minimal and coherent update of the prior, incorporating soft evidence on Euclidean distances while harnessing the prior’s useful representation of local structure. The J-condition is illustrated for a concrete protein example in Appendix 10, and some practical aspects of AF1’s application of PK are discussed in Appendix 11.

AF1 predictions are obtained by gradient descent minimization in the space of the dihedral angles, ϕ, ψ . This amounts to a maximum a posteriori (MAP) estimate obtained from the compositional empirical Bayes model constructed using PK. However, in contrast to PMF-based heuristics and point estimate prediction, PK allows the formulation of well-defined posterior distributions, as we demonstrate in the next section using a tractable synthetic model.

5 Experiments

Motivation To demonstrate PK in a way relevant to protein structure prediction, we formulate a synthetic model that by design has many crucial properties in common with the AF1 case. For both AF1 and the synthetic model, a generative model that specifies Euclidean coordinates based on an angular distribution is updated using distance evidence. Our experimental setup is *deliberately minimal* to demonstrate the feasibility and precision of PK updates in a tractable model, providing a bedrock for applications to more complex systems in future work, conditional on open solving problems such as formulating proper PDFs over distance matrices [15], which is beyond the scope of this article.

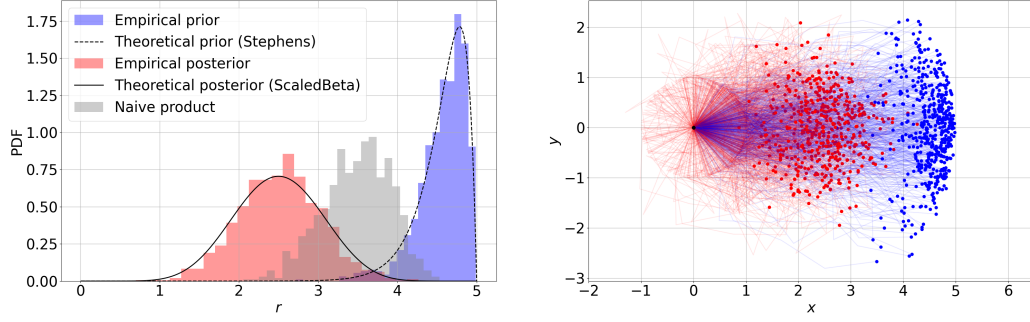


Figure 3: **Left:** Empirical PDFs of the origin-to-end distance, r , for the unmodified VRW prior (with $\mu = 0, \kappa = 10, N = 5$; blue histogram), the PK-updated VRW (red histogram), and a naive product of the ScaledBeta($\alpha = 10, \beta = 10, N = 5$) target distribution with the VRW prior, i.e., without dividing by the reference distribution (grey histogram). The latter does not fit the target distribution, clearly showing that the reference distribution is required. Also shown are the PDFs of the target ScaledBeta distribution (black line) and of the theoretical distribution for r (Stephens distribution; dashed line), showing an excellent fit in both cases. **Right:** 500 trajectories, $\mathbf{X}(\theta)$, sampled from the VRW prior (blue) and the PK-updated distribution (red). A dot denotes the end point of a random walk. As expected, the endpoints of the PK-updated distribution lie closer to the origin.

As prior, we use a von Mises random walk (VRW) in Euclidean 2D space. As coarse grained variable, we use the length of the *resultant vector*, that is, the distance between the origin and the end of the VRW, which has the advantage that its distribution is known [46, 63].

The similarities with AF1 will include the following elements: (a) both models make use of the von Mises distribution for a prior over angles, (b) the angles sampled from the von Mises distributions specify Euclidean coordinates that can be interpreted as atom positions, (c) subsequent atomic positions are at a given, fixed distance from each other, (d) the prior is updated with evidence concerning distances between a subset of the atoms, (e) the conditional PDF of angles given distances is not available, requiring the use of PK's RR update given by (14), and (f) the updated atomic positions are less spatially extended than the prior (see Appendix 10).

Setup In this section, \mathbf{X} will be an $(N + 1) \times 2$ matrix of 2-dimensional coordinates, resulting from a VRW with N steps. The VRW with mean μ and concentration (i.e., inverse variance) κ is,

$$\begin{cases} \mathbf{X}_i = (0, 0), & i = 0 \\ \mathbf{X}_{i+1} = \mathbf{X}_i + \mathbf{v}(\theta_i), \theta_i \sim \text{vonMises}(\mu, \kappa), & 0 < i \leq N, \end{cases} \quad (21)$$

where $\theta = \{\theta_i\}_{i=1}^N$ are angles in $[-\pi, \pi]$ and $\mathbf{v}(\theta_i)$ is the corresponding 2D unit vector. The coordinates are fully determined by the angles, $\mathbf{X} = \mathbf{X}(\theta)$. For this case, an approximate PDF of the Euclidean distance between start and end of the VRW, i.e., the length of the resultant vector, $r(\mathbf{X}) = \|\mathbf{X}_0 - \mathbf{X}_N\|^2$, is given by Stephens (1969),

$$2N\gamma \left(1 - \frac{r}{N}\right) \sim \chi_{N-1}^2, \quad (22)$$

where $\frac{1}{\gamma} = \frac{1}{\kappa} + \frac{3}{8\kappa^2}$ [63]. For $\kappa \geq 4$, the approximation is excellent [63]. We will write $r \sim \text{Stephens}(r; \kappa, N)$. Note that the maximum value of r is N , since each step has unit length. We define the prior distribution $\pi_{\text{VRW}}(\theta; \mu, \kappa)$ as the generative model induced by the VRW. The marginal probability over r for this prior can be written as

$$\pi_{\text{VRW}}(r; \kappa, N) = \text{Stephens}(r; \kappa, N) = \int \delta(r - r(\theta)) \pi_{\text{VRW}}(\theta; \mu, \kappa, N) d\theta. \quad (23)$$

Note that r is a random variable, while $r(\theta)$ is the realization of r for a specific VRW with angles θ . Now, we will demonstrate how PK allows us to update the prior using soft information on the distribution of r . We wish to modify the distribution over trajectories such that the marginal

distribution of r/N follows a $\text{Beta}(\alpha, \beta)$ distribution² with given parameters (α, β) instead of $\text{Stephens}(r; \kappa)$. The *target distribution* over r thus becomes after applying the change of variable formula,

$$p(r; \alpha, \beta, N) = \frac{1}{N} \frac{1}{B(\alpha, \beta)} \left(\frac{r}{N}\right)^{\alpha-1} \left(1 - \frac{r}{N}\right)^{\beta-1}, \text{ with } 0 < r < N, \quad (24)$$

where $B(\alpha, \beta)$ is the standard normalization constant of the Beta distribution. We will write $r \sim \text{ScaledBeta}(r; \alpha, \beta, N)$. In order to apply PK, we assume by construction that the J-condition, $p(\theta | r) = \pi(\theta | r)$, holds. That is, prior $\pi_{\text{VRW}}(\theta)$ and posterior $p(\theta)$ share the same marginal with respect to r . We can apply PK to update the prior, following $p(\theta) = \int \pi_{\text{VRW}}(\theta | r) p(r) dr$, but the marginal $\pi_{\text{VRW}}(\theta | r)$ is not available in tractable form for a VRW. Therefore, as is the case for AF1, we use the RR update given by (14), making use of the fact that the marginal over r according to the prior is given by (22). The PK update has the following structure,

$$p(\theta) = \frac{p(r(\theta))}{\pi_{\text{VRW}}(r(\theta))} \pi_{\text{VRW}}(\theta), \quad (25)$$

which results in the final model,

$$p(\theta; \mu, \kappa, \alpha, \beta, N) = \frac{\text{ScaledBeta}(r(\theta); \alpha, \beta, N)}{\text{Stephens}(r(\theta); \kappa, N)} \pi_{\text{VRW}}(\theta; \mu, \kappa, N). \quad (26)$$

We sample from this model using the No U-Turn Sampler (NUTS) [29], as implemented in the deep probabilistic programming language Pyro [6], with default parameters. We use 1000 warm up and 1000 posterior samples, taking under one minute on a standard laptop with an Intel i7 CPU.

Results and evaluation We set $N = 5$ and $\mu = 0, \kappa = 10$ for the VRW, and $\text{ScaledBeta}(\alpha = 10, \beta = 10, N = 5)$ as target. Figure 3 visually confirms that the correct posterior is attained. To further evaluate the model, we compared the empirical distributions of r to the target distribution using the one-sample Kolmogorov–Smirnov (KS) test [68], including every fifth NUTS sample to reduce autocorrelation. Across 10 NUTS simulations, the KS statistic ranges from $D = 0.04$ to $D = 0.08$, with a corresponding median p-value of 0.41, indicating a good match.

Ablation experiment In contrast and as expected, a naive reweighing approach that omits the reference distribution produced a much poorer fit, with the KS statistic ranging from $D = 0.62$ to $D = 0.70$, and $p < 10^{-6}$ in all cases. The deviation is also very obvious visually (Figure 3, gray histogram). This ablation experiment confirms the importance of including the reference distribution.

6 Discussion

KBPs [58] were quantitatively explained by appealing to (14) by Hamelryck *et al.* [25, 47, 45, 67], and later recognized as an instance of PK [27]. However, these references predate AF1, and are unconnected to deep learning. Moreover, the connection between KBPs and PK, while formally sound, has remained virtually unexplored within the deep learning paradigm applied to biomolecular structure. To our knowledge, our work is the first to explain AF1 as an instance of PK.

Although PK is a well-defined concept in probability theory [32, 16, 33, 13, 48], as far as we know, it has seen almost no explicit adoption in deep models. Yu (2020) applies PK to training Bayesian neural networks using soft evidence [70]. More recently, Munk *et al.* (2023) applied PK to the incorporation of soft evidence in probabilistic models and stochastic simulators [50].

This work connects physics-inspired modeling, probabilistic reasoning, and deep learning, which are increasingly converging [18]. The success of AF1 and its roots in PK hint at a general approach to formulate deep models that are compositional [22, 6, 69]. This approach consists of updating an empirical Bayes prior concerning a fine-grained variable with soft evidence on a coarse-grained variable, both obtained from deep models. We point out that PK is agnostic regarding the nature of its components, bringing a wide range of deep generative models potentially within its scope [66].

²Note that as $r \in [0, N]$, we divide by N to be within the support of the Beta distribution.

7 Conclusions

We reinterpreted AF1 as an instance of PK rather than as a thermodynamic potential, and demonstrated the probabilistic framework using a synthetic model that allows qualitative evaluation. Beyond clarifying the foundations of a paradigm-shifting method, our reinterpretation and AF1’s well-established accomplishments imply that PK offers a principled, quantitative foundation for building compositional deep probabilistic models based on generalized Bayesian updating [22, 6, 69].

8 Acknowledgments

The authors thank Wouter Boomsma, Jesper Ferkinghoff-Borg, Jes Frellsen, Carsten Hartmann, John Kent, Ola Rønning, Manfred Sippl and Sandy Zabell for discussions and comments, and acknowledge funding from the VILLUM Experiment Programme (grant 50240).

References

- [1] J. Abramson, J. Adler, J. Dunger, R. Evans, T. Green, A. Pritzel, O. Ronneberger, L. Willmore, A. J. Ballard, J. Bambrick, et al. Accurate structure prediction of biomolecular interactions with AlphaFold3. *Nature*, 630:493–500, 2024.
- [2] V. Agarwal and A. C. McShan. The power and pitfalls of AlphaFold2 for structure prediction beyond rigid globular proteins. *Nature Chemical Biology*, 20:950–959, 2024.
- [3] B. Armendt. Is there a Dutch book argument for probability kinematics? *Philosophy of Science*, 47:583–588, 1980.
- [4] M. Arts, J. Frellsen, and W. Boomsma. Internal-coordinate density modelling of protein structure: Covariance matters. *Transactions on Machine Learning Research*, 2024.
- [5] A. Ben-Naim. Statistical potentials extracted from protein structures: Are these meaningful potentials? *Journal of Chemical Physics*, 107:3698–3706, 1997.
- [6] E. Bingham, J. P. Chen, M. Jankowiak, F. Obermeyer, N. Pradhan, T. Karaletsos, R. Singh, P. Szerlip, P. Horsfall, and N. D. Goodman. Pyro: Deep universal probabilistic programming. *Journal of Machine Learning Research*, 20:1–6, 2019.
- [7] D. M. Blei, A. Kucukelbir, and J. D. McAuliffe. Variational inference: A review for statisticians. *Journal of the American Statistical Association*, 112:859–877, 2017.
- [8] W. Boomsma, K. Mardia, C. Taylor, J. Ferkinghoff-Borg, A. Krogh, and T. Hamelryck. A generative, probabilistic model of local protein structure. *Proceedings of the National Academy USA*, 105:8932–8937, 2008.
- [9] G. R. Bowman. AlphaFold and protein folding: Not dead yet! The frontier is conformational ensembles. *Annual Review of Biomedical Data Science*, 7:51–57, 2024.
- [10] E. Callaway. Chemistry Nobel goes to developers of AlphaFold AI that predicts protein structures. *Nature*, 634:525–526, 2024.
- [11] D. Chakravarty, J. W. Schafer, E. A. Chen, J. F. Thole, L. A. Ronish, M. Lee, and L. L. Porter. AlphaFold predictions of fold-switched conformations are driven by structure memorization. *Nature Communications*, 15:7296, 2024.
- [12] D. Chakravarty, M. Lee, and L. L. Porter. Proteins with alternative folds reveal blind spots in AlphaFold-based protein structure prediction. *Current Opinion in Structural Biology*, 90: 102973, 2025.
- [13] H. Chan and A. Darwiche. On the revision of probabilistic beliefs using uncertain evidence. *Artificial Intelligence*, 163:67–90, 2005.
- [14] D. Chandler. *Introduction to Modern Statistical Mechanics*. Oxford University Press, 1987.
- [15] P. Clifford and N. Green. Distances in Gaussian point sets. In *Mathematical Proceedings of the Cambridge Philosophical Society*, volume 97, pages 515–524. Cambridge University Press, 1985.
- [16] P. Diaconis and S. L. Zabell. Updating subjective probability. *Journal of the American Statistical Association*, 77:822–830, 1982.
- [17] K. Dill and J. MacCallum. The protein-folding problem, 50 years on. *Science*, 338:1042–1046, 2012.
- [18] A. E. Durumeric, N. E. Charron, C. Templeton, F. Musil, K. Bonneau, A. S. Pasos-Trejo, Y. Chen, A. Kelkar, F. Noé, and C. Clementi. Machine learned coarse-grained protein force-fields: Are we there yet? *Current Opinion in Structural Biology*, 79:102533, 2023.
- [19] T. Edgoose, L. Allison, and D. Dowe. An MML classification of protein structure that knows about angles and sequence. In *Pacific Symposium on Biocomputing*, pages 585–596, 1998.

- [20] A. V. Finkelstein, A. Y. Badretdinov, and A. M. Gutin. Why do protein architectures have Boltzmann-like statistics? *Proteins: Structure, Function, and Bioinformatics*, 23:142–150, 1995.
- [21] J. Gavalda-Garcia, B. Dixit, A. Díaz, A. Ghysels, and W. Vranken. Gradations in protein dynamics captured by experimental NMR are not well represented by AlphaFold2 models and other computational metrics. *Journal of Molecular Biology*, 437:168900, 2025.
- [22] Z. Ghahramani. Probabilistic machine learning and artificial intelligence. *Nature*, 521:452–459, 2015.
- [23] H. Gong, P. J. Fleming, and G. D. Rose. Building native protein conformation from highly approximate backbone torsion angles. *Proceedings of the National Academy of Sciences*, 102:16227–16232, 2005.
- [24] T. Hamelryck, J. Kent, and A. Krogh. Sampling realistic protein conformations using local structural bias. *PLoS Computational Biology*, 2(9):e131, 2006.
- [25] T. Hamelryck, M. Borg, M. Paluszewski, J. Paulsen, J. Frellsen, C. Andreetta, W. Boomsma, S. Bottaro, and J. Ferkinghoff-Borg. Potentials of mean force for protein structure prediction vindicated, formalized and generalized. *PLoS ONE*, 5:e13714, 2010.
- [26] T. Hamelryck, K. V. Mardia, and J. Ferkinghoff-Borg, editors. *Bayesian Methods in Structural Bioinformatics*. Springer, 2012.
- [27] T. Hamelryck, W. Boomsma, J. Ferkinghoff-Borg, J. Foldager, J. Frellsen, J. Haslett, and D. Theobald. Proteins, physics and probability kinematics: A Bayesian formulation of the protein folding problem. In I. Dryden and J. Kent, editors, *Geometry Driven Statistics*, pages 356–376. Wiley, 2015.
- [28] C. Hartmann, J. C. Latorre, and G. Ciccotti. On two possible definitions of the free energy for collective variables. *European Physical Journal Special Topics*, 200:73–89, 2011.
- [29] M. D. Hoffman and A. Gelman. The No-U-Turn sampler: Adaptively setting path lengths in Hamiltonian Monte Carlo. *Journal of Machine Learning Research*, 15:1593–1623, 2014.
- [30] J. B. Holmes and J. Tsai. Some fundamental aspects of building protein structures from fragment libraries. *Protein Science*, 13:1636–1650, 2004.
- [31] R. C. Jeffrey. *Contributions to the theory of inductive probability*. PhD thesis, Princeton University, 1957.
- [32] R. C. Jeffrey. *The logic of decision*. The University of Chicago Press, 2nd edition, 1990. Originally published in 1965 by McGraw-Hill.
- [33] R. C. Jeffrey. *Subjective probability: The real thing*. Cambridge University Press, 2004.
- [34] J. Jumper, R. Evans, A. Pritzel, T. Green, M. Figurnov, O. Ronneberger, K. Tunyasuvunakool, R. Bates, A. Židek, A. Potapenko, et al. Highly accurate protein structure prediction with AlphaFold. *Nature*, 596:583–589, 2021.
- [35] W. Kabsch. A solution for the best rotation to relate two sets of vectors. *Acta Crystallographica A*, 32:922–923, 1976.
- [36] D. P. Kingma and M. Welling. An introduction to variational autoencoders. *Foundations and Trends in Machine Learning*, 12:307–392, 2019.
- [37] J. G. Kirkwood. Statistical mechanics of fluid mixtures. *Journal of Chemical Physics*, 3: 300–313, 1935.
- [38] W. A. Koppensteiner and M. J. Sippl. Knowledge-based potentials – Back to the roots. *Biochemistry (Moscow)*, 63:247–252, 1998.

- [39] K. P. Lennox, D. B. Dahl, M. Vannucci, and J. W. Tsai. Density estimation for protein conformation angles using a bivariate von Mises distribution and Bayesian nonparametrics. *Journal of the American Statistical Association*, 104:586–596, 2009.
- [40] K. P. Lennox, D. B. Dahl, M. Vannucci, R. Day, and J. W. Tsai. A Dirichlet process mixture of hidden Markov models for protein structure prediction. *Annals of Applied Statistics*, 4:916, 2010.
- [41] C. Ley and T. Verdebout. *Modern Directional Statistics*. Chapman and Hall/CRC, 2017.
- [42] J. López-Sagaseta and A. Urdiciain. Severe deviation in protein fold prediction by advanced AI: A case study. *Scientific Reports*, 15:4778, 2025.
- [43] K. V. Mardia. Fisher’s legacy of directional statistics, and beyond to statistics on manifolds. *Journal of Multivariate Analysis*, 207:105404, 2025.
- [44] K. V. Mardia. Profile: Kanti Mardia. *Significance*, 22:36–38, 2025.
- [45] K. V. Mardia and T. Hamelryck. On ‘Constructing summary statistics for approximate Bayesian computation: Semi-automatic approximate Bayesian computation’ by P. Fearnhead and D. Prangle. *Journal of the Royal Statistical Society: Series B (Statistical Methodology)*, 74:462–463, 2012. Discussion.
- [46] K. V. Mardia and P. E. Jupp. *Directional statistics*. John Wiley & Sons, 2009.
- [47] K. V. Mardia, J. Frellsen, M. Borg, J. Ferkinghoff-Borg, and T. Hamelryck. A statistical view on the reference ratio method. In *LASR 2011 Proceedings*, pages 55–61. Leeds University Press, 2011.
- [48] A. Meehan and S. Zhang. Jeffrey meets Kolmogorov: A general theory of conditioning. *Journal of Philosophical Logic*, 49:941–979, 2020.
- [49] S. Miyazawa and R. L. Jernigan. Estimation of effective interresidue contact energies from protein crystal structures: Quasi-chemical approximation. *Macromolecules*, 18:534–552, 1985.
- [50] A. Munk, A. Mead, and F. Wood. Uncertain evidence in probabilistic models and stochastic simulators. In *International Conference on Machine Learning (ICML)*, pages 25486–25500, 2023.
- [51] A. Pewsey and E. García-Portugués. Recent advances in directional statistics. *TEST*, 30:1–58, 2021.
- [52] F. M. Pohl. Empirical protein energy maps. *Nature New Biology*, 234:277–279, 1971.
- [53] P. Ramasamy, J. Zuallaert, L. Martens, and W. F. Vranken. Assessing the relation between protein phosphorylation, AlphaFold3 models and conformational variability. *preprint bioRxiv*, 2025.
- [54] Schrödinger, LLC. The PyMOL molecular graphics system, Version 3.0.0. Available at <https://pymol.org/>, 2015.
- [55] A. W. Senior, R. Evans, J. Jumper, J. Kirkpatrick, L. Sifre, T. Green, C. Qin, A. Židek, A. W. Nelson, A. Bridgland, et al. Protein structure prediction using multiple deep neural networks in the 13th Critical Assessment of Protein Structure Prediction (CASP13). *Proteins: Structure, Function, and Bioinformatics*, 87:1141–1148, 2019.
- [56] A. W. Senior, R. Evans, J. Jumper, J. Kirkpatrick, L. Sifre, T. Green, C. Qin, A. Židek, A. W. Nelson, A. Bridgland, et al. Improved protein structure prediction using potentials from deep learning. *Nature*, 577:706–710, 2020.
- [57] K. T. Simons, C. Kooperberg, E. Huang, and D. Baker. Assembly of protein tertiary structures from fragments with similar local sequences using simulated annealing and Bayesian scoring functions. *Journal of Molecular Biology*, 268:209–225, 1997.

- [58] M. J. Sippl. Calculation of conformational ensembles from potentials of mean force. An approach to the knowledge-based prediction of local structures in globular proteins. *Journal of Molecular Biology*, 213:859–883, 1990.
- [59] M. J. Sippl. Boltzmann’s principle, knowledge-based mean fields and protein folding. An approach to the computational determination of protein structures. *Journal of Computer-Aided Molecular Design*, 7:473–501, 1993.
- [60] M. J. Sippl. Recognition of errors in three-dimensional structures of proteins. *Proteins: Structure, Function, and Bioinformatics*, 17:355–362, 1993.
- [61] M. J. Sippl. Knowledge-based potentials for proteins. *Current Opinion in Structural Biology*, 5: 229–235, 1995.
- [62] M. J. Sippl, M. Ortner, M. Jaritz, P. Lackner, and H. Flöckner. Helmholtz free energies of atom pair interactions in proteins. *Folding and Design*, 1:289–298, 1996.
- [63] M. A. Stephens. Tests for the von Mises distribution. *Biometrika*, 56:149–160, 1969.
- [64] S. Tanaka and H. A. Scheraga. Medium-and long-range interaction parameters between amino acids for predicting three-dimensional structures of proteins. *Macromolecules*, 9:945–950, 1976.
- [65] P. D. Thomas and K. A. Dill. Statistical potentials extracted from protein structures: How accurate are they? *Journal of Molecular Biology*, 257:457–469, 1996.
- [66] J. M. Tomczak. *Deep generative modeling*. Springer, 2nd edition, 2024.
- [67] J. B. Valentin, C. Andreetta, W. Boomsma, S. Bottaro, J. Ferkinghoff-Borg, J. Frellsen, K. V. Mardia, P. Tian, and T. Hamelryck. Formulation of probabilistic models of protein structure in atomic detail using the reference ratio method. *Proteins: Structure, Function, and Bioinformatics*, 82:288–299, 2014.
- [68] P. Virtanen, R. Gommers, T. E. Oliphant, M. Haberland, T. Reddy, D. Cournapeau, E. Burovski, P. Peterson, W. Weckesser, J. Bright, et al. SciPy 1.0: Fundamental algorithms for scientific computing in Python. *Nature Methods*, 17:261–272, 2020.
- [69] F. Wood, J. W. Meent, and V. Mansinghka. A new approach to probabilistic programming inference. In *Artificial Intelligence and Statistics (AISTATS)*, pages 1024–1032. PMLR, 2014.
- [70] E. Yu. Bayesian neural networks with soft evidence. *preprint arXiv:2010.09570*, 2020.
- [71] F. Zhao, J. Peng, J. DeBartolo, K. Freed, T. Sosnick, and J. Xu. A probabilistic and continuous model of protein conformational space for template-free modeling. *Journal of Computational Biology*, 17:783–798, 2010.
- [72] D. M. Zuckerman. *Statistical physics of biomolecules: An introduction*. CRC press, 2010.

Appendix

9 Example: Whitworth’s horses

This simple application of PK is discussed by Diaconis and Zabell [16]. Three horses, A, B, and C, have prior winning probabilities $\pi(A) = 1/2$, $\pi(B) = 1/4$, and $\pi(C) = 1/4$, respectively. New evidence increases the probability of A winning from $\pi(A) = 1/2$ to $p(A) = 2/3$, without providing any further information on the other horses. Standard Bayesian conditioning cannot apply, as no specific event has occurred. Instead, PK prescribes an update that satisfies the new marginal, $p(A) = 2/3$, while preserving the conditional probabilities, $p(B | A) = p(C | A) = 1/2$. This yields the updated posterior probabilities, $p(A) = 2/3$, $p(\sim A) = 1/3$, and

$$p(B) = p(C) = p(B | \sim A)p(\sim A) = p(C | \sim A)p(\sim A) = 1/2 * 1/3 = 1/6, \quad (27)$$

while previously $\pi(B) = \pi(C) = 1/4$.

10 Local nature of the prior and J-condition

Motivation As the dihedral angles are sufficient to generate 3D structures, one might ask why it is necessary to add evidence on pairwise distances. It is well known that probabilistic models based on internal coordinates, such as dihedral angles, struggle to reproduce realistic distances between amino acids that are far apart in sequence position [4]. This is due to the highly structured covariance induced by the chain geometry: small local perturbations in dihedral angles propagate in a correlated way through the backbone.

Experiments To illustrate this in the context of AF1, we sampled dihedral angles from the prior and reconstructed the corresponding 3D coordinates. AF1 code that can be executed for CASP13 targets is available from GitHub.³ AF1 was applied to CASP13 target TS1019s2, corresponding to the PT-VEEN domain-containing protein, Protein Data Bank Identifier 8EY4, chain B. For each amino acid, the prior is specified as probabilities over the Ramachandran plot, binned at $10^\circ \times 10^\circ$ resolution, obtained from a deep model (see Section 4) [56]. For each amino acid, we picked a random bin according to the specified probabilities, and set the dihedral angles to the bin’s centroid. We then construct the 3D coordinates of the $N, C\alpha, C$ backbone from the sampled dihedral angles. The sampled structures were superimposed on the true structure using a standard algorithm [35]. Both prior probabilities and sampled 3D structures are available as supplementary material in the ZIP file (see README file).

Results and discussion Averaging over 100 sampled 3D structures, we visualized the resulting $C\alpha - C\alpha$ distogram and compared it to that of the native structure (see Figure 4). The prior captures distances between residues that are close together in the sequence well (i.e., close to the diagonal in Figure 4), but fails to produce correct distances for the other cases, generating structures that are insufficiently compact. This is also visible in Figure 5, where the ensemble of 3D structures sampled from the AF1 prior deviates significantly from the compact, folded conformation. This result illustrates AF1’s adopted J-condition, $p(\phi, \psi | D) = \pi(\phi, \psi | D)$, and the corresponding PK update, which performs the minimal perturbation of the locally valid prior necessary to match the marginal distribution over the distances, $p(D)$.

11 Practical aspects of the AF1 potential

Our statistical framework explains AF1’s potential as the update of a prior over dihedral angles with information on pairwise distances. For practical reasons, the application of PK by AF1 is heuristic in a few respects, which we clarify here. First, the reference distribution over the coarse grained variable, $\pi(D(\phi, \psi); F)$, is not directly obtained from the prior over the fine-grained variable, $\pi(\phi, \psi; \Theta)$. Rather, it is approximated by training a model that uses as input only the sequence length, L , and vector specifying the position of the Glycine residues.

³https://github.com/google-deepmind/deepmind-research/tree/master/alphafold_casp13

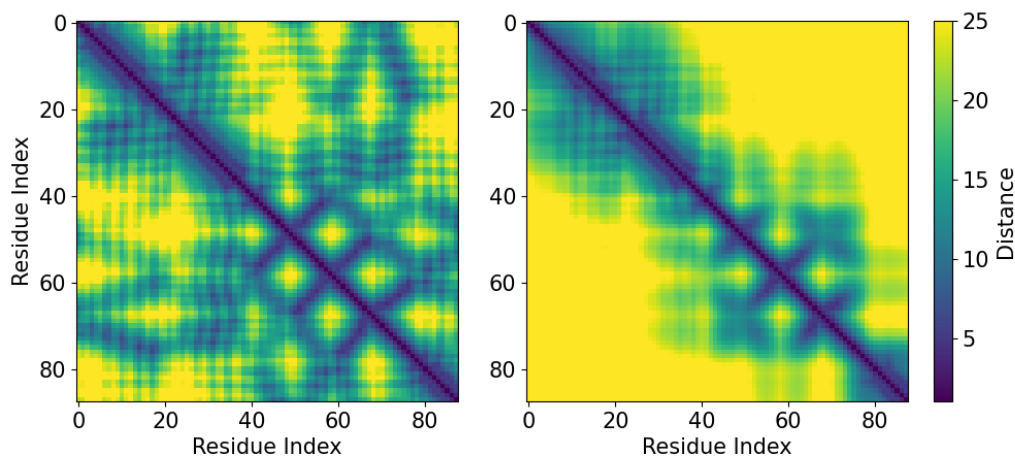


Figure 4: Distogram of the native structure (**left**) and the averaged distogram over 100 samples from the AF1 prior (**right**) for the PT-VENN domain-containing protein (Protein Data Bank Identifier 8EY4, Chain B). Distances are in Ångström.

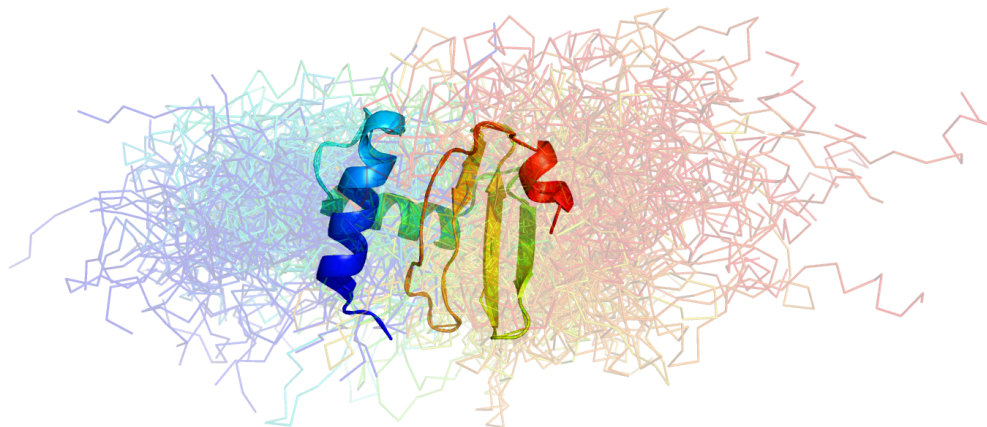


Figure 5: 100 samples from the AF1 prior (transparent, thin ribbons) superimposed on the cartoon representation of the native structure of the PT-VENN domain-containing protein (Protein Data Bank Identifier 8EY4, Chain B). In all cases, the N-terminus is shown in blue and C-terminus in red. Figure made with PyMol [54].

Second, AF1 does not use proper PDFs over the distance matrix, \mathbf{D} . For n points in \mathbb{R}^d , the $n(n-1)/2$ pairwise distances cannot vary independently: they must satisfy geometric constraints to correspond to an embeddable configuration. As discussed by Clifford and Green (1985) [15], valid distances lie on a smaller manifold of dimension $nd - d(d+1)/2$. By modeling probability distribution over \mathbf{D} as a product of independent marginals, AF1 defines an approximate distribution that is *singular*, i.e., it may place nonzero density on geometrically invalid configurations.

These choices reflect pragmatic compromises that ultimately preserve the core principle of PK: updating a prior distribution concerning a fine-grained variable using soft evidence on a coarse-grained variable. In addition, minimization of the AF1 potential as a function of the dihedral angles ensures realizable 3D coordinates and a corresponding valid distance matrix.